



Article

Transcriptome Analysis Provides Insights into Anthocyanin Synthesis in Blueberry

Zhaohui Mu ^{1,†}, Yuchun Yang ^{2,†}, Ayimgul Yusuyin ¹, Yige Xu ², Hui Yuan ^{1,*} and Cheng Liu ^{2,*}

¹ College of Horticulture, Shenyang Agricultural University, Shenyang 110866, China; muzhaohui3815@163.com (Z.M.); ayimgulyusuyin@163.com (A.Y.)

² Liaoning Institute of Pomology, Yingkou 115009, China; yangyuchunhc@163.com (Y.Y.); yigoxu@163.com (Y.X.)

* Correspondence: huiyuan@syau.edu.cn (H.Y.); stevecliu@hotmail.com (C.L.)

† These authors contributed equally to this work.

Abstract: Blueberry (*Vaccinium* spp.) is a popular fruit providing health benefits to humans, mainly because the fruit is rich in anthocyanins. Normally, the mature fruits of blueberry are fully blue, but we found a striped type in 'Xilai' blueberry. This study aimed to clarify the mechanisms underlying striped color mutations. We used transcriptome analysis to screen differentially expressed genes (DEGs) between the different stripes. A total of 2234 DEGs were identified in light stripes compared to dark stripes, among which 1023 genes were upregulated and 1213 genes were downregulated. These DEGs were related to anthocyanin synthesis, including phenylpropyl, flavonoid, and flavonol synthesis. Six DEGs (CHI, DFR, 4CL, CHS, F3H, and ANS) and six differentially expressed transcription factors (bHLH, MYB, and WD40 families) were selected for an investigation of the expression patterns of 12 DEGs related to anthocyanin synthesis in the two different striped blueberry peels using real-time quantitative polymerase chain reaction (qRT-PCR). Anthocyanin content and expression levels of transcription factors related to anthocyanin synthesis were higher in dark than in light stripes. This study enriches the available transcriptome information on blueberries and provides a scientific basis for further revealing the molecular mechanisms related to the coloring of blueberry peel, cloning, and expression of growth-related genes.

Keywords: blueberry; striped color mutation; anthocyanin; qRT-PCR; differentially expressed genes



Citation: Mu, Z.; Yang, Y.; Yusuyin, A.; Xu, Y.; Yuan, H.; Liu, C.

Transcriptome Analysis Provides Insights into Anthocyanin Synthesis in Blueberry. *Horticulturae* **2023**, *9*, 1036. <https://doi.org/10.3390/horticulturae9091036>

Academic Editor: Michailidis Michail

Received: 9 August 2023

Revised: 8 September 2023

Accepted: 12 September 2023

Published: 14 September 2023



Copyright: © 2023 by the authors. Licensee MDPI, Basel, Switzerland. This article is an open access article distributed under the terms and conditions of the Creative Commons Attribution (CC BY) license (<https://creativecommons.org/licenses/by/4.0/>).

1. Introduction

Blueberries (*Vaccinium* spp.) are recognized as one of the five main health foods by the Food and Agriculture Organization of the United Nations and are one of the most important small fruit cash crops worldwide [1]. Due to their unique taste and high content of antioxidants, blueberries are very popular among consumers [2,3]. Blueberries are known to contain high levels of vitamins A and C, dietary fiber, and magnesium, as well as many bioactive phenolic compounds, including anthocyanins [4]. The fruit color of blueberry is a very important agronomic trait and is of great significance for the commodity value and market competitiveness of fruits [5].

Anthocyanins are widely distributed in various organs and tissues of the plants, including flowers and fruits [6], and they have important effects on plant physiology. The basic structure of the anthocyanins is α -phenyl-benzopyrane, which is a C6-C3-C6 carbon skeleton structure. The methylation and hydroxylation at different positions of the skeleton structure decide different colors of the plant skin [7–9]. It is reported that there are 650 kinds of anthocyanins in nature, however, the most common are six kinds of anthocyanins, namely pelargonidin, cyanidin, delphinidin, peonidin, petunidin, and malvidin [10].

Anthocyanins are pigments that impart surface color to blueberry fruits and are one of the main bioactive compounds found in blueberries [11–13]. Anthocyanins account

for 60–70% of the total phenolic substances [14–17], and the biological activity of anthocyanins is widely recognized. The biosynthetic pathways of anthocyanins have been demonstrated in other plants [18]. Anthocyanin biosynthesis is a branch of the flavonoid metabolic pathway, and its key enzyme-encoding genes include chalcone synthase (CHS), chalcone isomerase (CHI), flavanone 3-hydroxylase (F3H), flavonoid-3'-hydroxylase (F3'H), dihydroflavonol-4-reductase (DFR), and anthocyanin synthase (ANS) [19]. Subsequently, anthocyanin synthase (ANS) and colorless anthocyanin dioxygenase (LDOX) catalyze the conversion of colorless anthocyanins and catechins to anthocyanins [20], which are then converted to colored anthocyanins via the flavonoid pathway [21]. The appearance of fruit streaks is a key factor in determining the quality of some fruits and directly affects their commercial market value [22]. For example, most consumers prefer watermelon varieties with bright green skins and heavy stripes. A striped pattern is usually visible in the longitudinal direction, which is a common naturally occurring phenomenon [23]. A differential expression of *MdMYB10* causes red and green stripes in apple peels, which are favored by New Zealand consumers [24].

In this study, we found a blueberry with different stripes; however, the cause of this phenomenon is unknown. In order to explore the molecular mechanism of pericarp stripe formation in blueberry, transcriptome sequencing was used to obtain the transcription factors and key structural genes that control pericarp coloring. The expression level of the gene was further detected using qRT-PCR, which provided scientific basis for further study of the molecular mechanism of blueberry pericarp coloring.

2. Materials and Methods

2.1. Plant Materials

'Xilai' blueberries were collected from Liaoning Haoyuan Agricultural Technology Co., Ltd. (Sui Zhong, Liaoning Province, China) in 2021. One hundred even-sized, pest-free, ripe blueberries were picked and immediately transported to the laboratory. Subsequently, 90 blueberries were randomly selected and evenly divided into three portions of 30 blueberries each. Finally, the dark and light stripes on the surface of the blueberry were separated from flesh, and the separated dark and light striped skins were quickly refrigerated in liquid nitrogen at -80°C , respectively.

2.2. Anthocyanin Content Determination

The total anthocyanin contents of the dark and light stripes were measured as previously described [25]. In a dark place and at low temperature, the dark and light stripes of the blueberry peels were incubated in 1% (*v/v*) hydrochloric-methanol for 24 h. Then, 3 mL of the supernatant was poured into cuvettes. Its absorbance was measured using a spectrophotometer at wavelengths of 530, 620, and 650 nm, respectively, and the anthocyanin content was computed according to Equation (1) [26]:

$$\text{Anthocyanin content (nmol g}^{-1}\text{ FW)} = [(OD_{530} - OD_{620}) - 0.1 \times (OD_{650} - OD_{620})] / \epsilon \times V / M \times 10^6 \quad (1)$$

where *V* is the liquid volume, *M* is the plant tissue weight, and the total anthocyanin absorbance index is 4.62×10^4 . The average of the three tests was calculated.

2.3. RNA Extraction, Library Preparation, and RNA Sequencing

RNA-seq was used to analyze the blueberry peel genes 60 days after flowering, and the test was performed twice to ensure accuracy of the results. Total RNA was isolated and purified using the TRIzol reagent (Invitrogen, Carlsbad, CA, USA) according to the manufacturer's instructions. The RNA content and purity of each sample were quantified using NanoDrop ND-1000 (NanoDrop, Wilmington, DE, USA). RNA integrity (RIN > 7.0) was determined using a Bioanalyzer 2100 (Agilent, Santa Clara, CA, USA) and confirmed via denatured agarose gel electrophoresis. Poly(A)mRNA was purified from two micrograms of total RNA by dynamic oligomeric magnetic beads. The mRNAs were cut into small fragments using divalent magnesium ions under high-temperature conditions. The

KC-Digital™ Stranded mRNA Library Prep Kit (Illumina, San Diego, CA, USA) was used to reverse-transcribe the cleaved RNA fragments and construct the final cDNA library. Paired sequencing (PE150) of 2×150 bp was performed on an Illumina NovaSeq™6000 (Wuhan SecCO Co., Ltd., Wuhan, China) according to the vendor's recommended method.

2.4. Bioinformatics Analysis

Raw sequencing data were converted into valid readings after processing. 2StringTie calculated mRNAs expression levels by calculating FPKMS, while RPKMs was calculated using featureCounts. The DEGs between the control and treatment groups were identified using the Edger software package. Differentially expressed transcripts were screened with \log_2 (multiple change) > 1 or \log_2 (multiple change) < -1 , which was statistically significant ($p < 0.05$). Path analyses of the GO and KEGG enrichment were based on the Gene Ontology Database 3 and KEGG pathway 4, respectively.

2.5. qRT-PCR Analysis

The total RNA was extracted via qRT-PCR analysis [27]. Total RNA (800 ng) was extracted using a PrimeScript First Strand gene synthesis kit (Takara, Kusatsu, Japan), and the first-strand gene was synthesized. qRT-PCR was performed as previously described [28]. Specific primers for each gene were designed using Primer3. The primers used in this study are listed in Table S1. The known *VcUBQ* was used as an internal control. All experiments were conducted in triplicates.

2.6. Statistical Analysis

The qRT-PCR and physiological determination data were analyzed using Microsoft EXCEL 2010 software, and the mean values are expressed as means \pm SE. Statistical significance at * $p < 0.05$, ** $p < 0.01$ was tested using Student's *t*-test. The correlation between the dark and light stripe gene expression levels was explored using Pearson's correlation coefficient. The similarity between samples can be expressed by correlation coefficient, that is, the closer the correlation coefficient is to 1, the higher the similarity of expression patterns between samples. All data were compiled using Origin 2016.

3. Results

3.1. Dark Blueberry Skin Had Higher Anthocyanin Accumulation than Light Stripe Skin

In Haoyuan Agriculture, we discovered a new variety of blueberries with dark and light stripes (Figure 1A). Seven years of observation, from 2016 to 2022, indicated that these striped blueberries had stable genetic properties that ruled out environmental influences. To investigate the mechanism underlying the coloring difference between these two stripes, the total anthocyanin contents were measured in the dark and light stripes. The anthocyanin content in the dark stripes was significantly higher than that in the light stripes, as shown in Figure 1B.

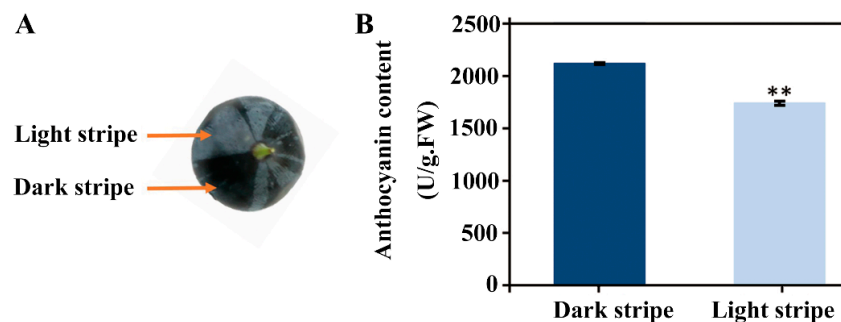


Figure 1. Experimental materials (A). Total anthocyanin content in dark and light stripes of new strains of blueberry (B). Asterisks indicate significant difference as determined via Student's *t*-test (**, $p < 0.01$).

3.2. RNA-seq Technique and Analysis of DEGs in Blueberry Peel

To investigate the molecular mechanism underlying the color difference between the dark and light stripes, RNA-seq analysis was performed. Four libraries were established (with two biological replicates per sample), and 47,031,570, 46,604,328, 44,632,796, and 45,747,804 raw reads were obtained. Unreliable raw read data and noncarrier errors were excluded to obtain high-quality, clear, and valid read data. Finally, 44,329,956, 45,159,371, 41,859,650, and 44,047,046 clean reads were obtained. In addition, the valid reads were compared to the reference genome using HISAT 2 software, which showed that the values of the mapped reads ranged from 90.25 to 90.84%. In the light and dark stripes of the blueberry peel, the highest percentage of sequences was located in the exonic regions, based on the regional information of the reference genome, as shown in Figure 2A,B.

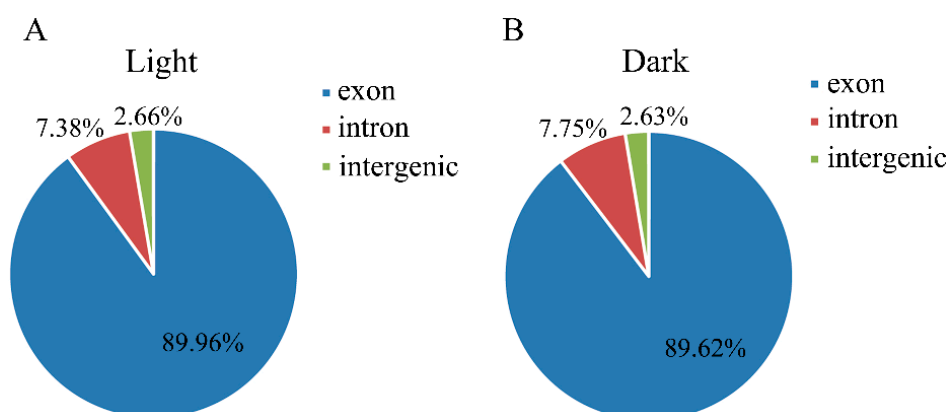


Figure 2. Classification of annotation areas for RNA-seq and DEGs analysis of blueberry peel in 2021 years. Classification of annotation area for RNA-seq and DEGs analysis of light stripe peel (A). Classification of annotation area for RNA-seq and DEGs analysis of dark stripe peel (B).

Gene expression levels were measured as reads per kilobase per Million Reads (RPKM). According to the RNA-seq analysis, the moderately expressed unigenes in light and dark stripes accounted for the majority of the area under the curve (AUC), and the lower- or higher-expressed unigenes accounted for a minority of the AUC as shown in Figure 3. In Figure 3, by combining the horizontal and vertical coordinates, it can be seen that a small part of unigenes in RPKM ranges from -2.5 to $2.5-5.0$. In addition, it can also be seen that the expression of the unigenes was slightly higher in the light stripes than in the dark stripes. The degree of the dispersion of the unigenes in the dark stripes was slightly higher than that in the light stripes, as shown more intuitively in the result in Figure S1.

The number of DEGs in the dark and light stripes was determined using two RNA-seq analyses (Figure 4). The results revealed 5262 and 1608 DEGs, respectively. The 2688 genes were upregulated and 4182 genes were downregulated, as shown in Figure 4A,B. Figure S2A,B show the volcano plots of the differential genes, which also show the number of DEGs in the dark and light stripes.

The Spearman correlation between the dark and light stripe gene expression levels was found to be higher than 0.92, as shown in Figure 5. We concluded that the genes for the dark and light stripes were highly similar. These results are consistent with those obtained for blueberry peel.

Compared to the gene expression in the dark stripe in the KEGG pathway, genes with an increased expression in the light stripe were mainly enriched in the pathways of photosynthesis, carbon metabolism, and photosynthetic antenna proteins, as shown in Figure 6A, while genes with a decreased expression in the light stripe were mainly enriched in the pathways of plant hormone signal transduction, starch and sucrose metabolism, and plant–pathogen interaction, as shown in Figure 6B.

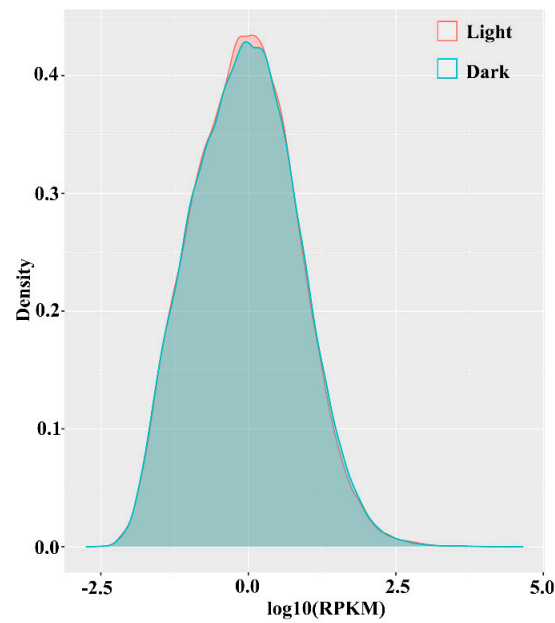


Figure 3. Comparison of RPKM value density distribution between dark and light stripes. The curves of different colors in the figure represent different samples. The horizontal coordinate of points on the curve represents the pair value of RPKM corresponding to the sample, and the vertical coordinate of points represents the probability density.

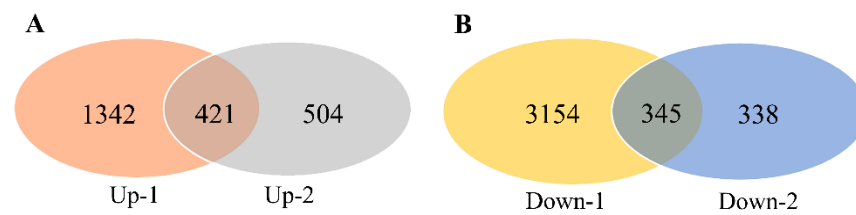


Figure 4. Venn diagram of DEGs co-upregulated through twice sequencing (A). Venn diagram of DEGs co-downregulated through twice sequencing (B).

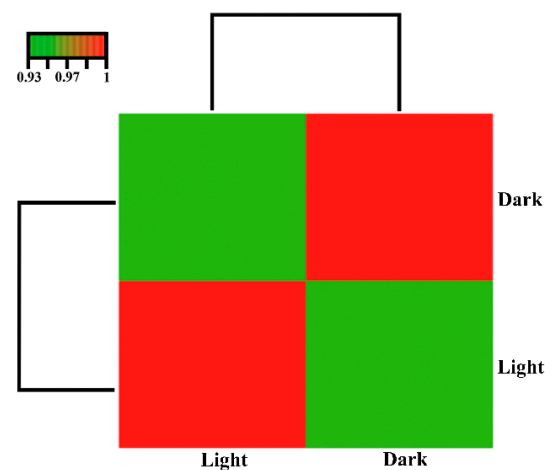


Figure 5. Hierarchical clustering of gene expression levels of samples. The color scale from green to red represents low and high intersample correlations based on gene expression levels.

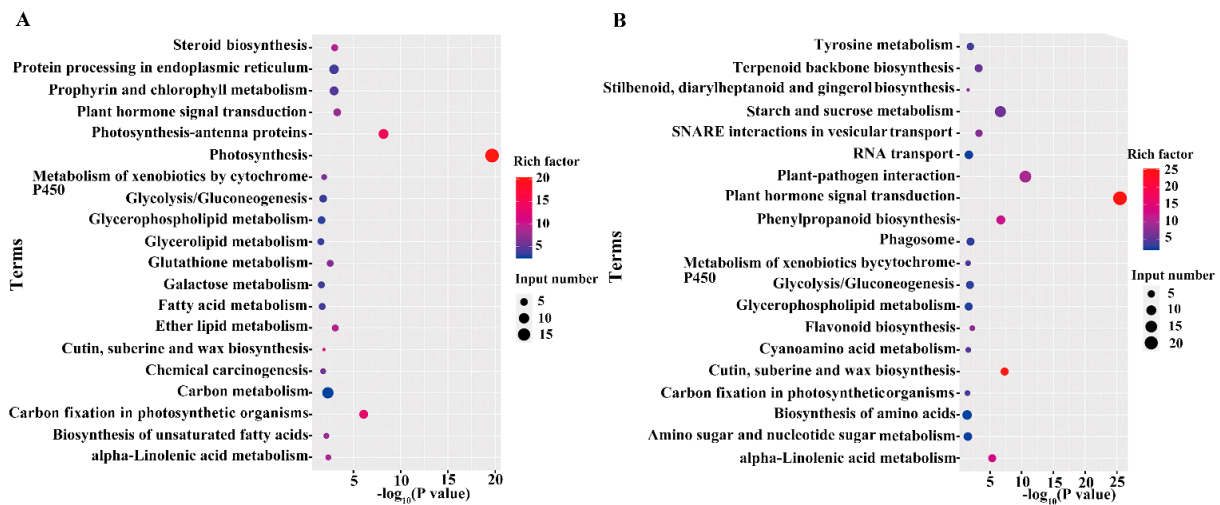


Figure 6. KEGG enrichment analysis of differentially expressed genes, (A) upregulated genes and (B) downregulated genes. The horizontal axis shows the enrichment significance, which is represented by $-\log_{10}(p \text{ value})$. The larger the value, the more significant the enrichment. The vertical axis shows the enriched KEGG pathway. Dot size represents the number of differential genes in the KEGG pathway, and dot depth represents the degree of rich factor enrichment. Here, the top 20 most significant KEGG pathways are plotted in p value order.

Gene ontology (Go) was used to analyze the functional enrichment of differential genes (Figure S3). Photosynthesis, plant type, cell wall organization, and plant type–cell wall organization or biogenesis were the most abundant molecular functions among those co-upregulated by both dark and light pericarp differentially expressed genes (Figure 7A). However, ubiquitin protein transferase and ubiquitin-like protein transferase activities were more abundant in biological processes among those co-downregulated by both dark and light differentially expressed genes (Figure 7B).

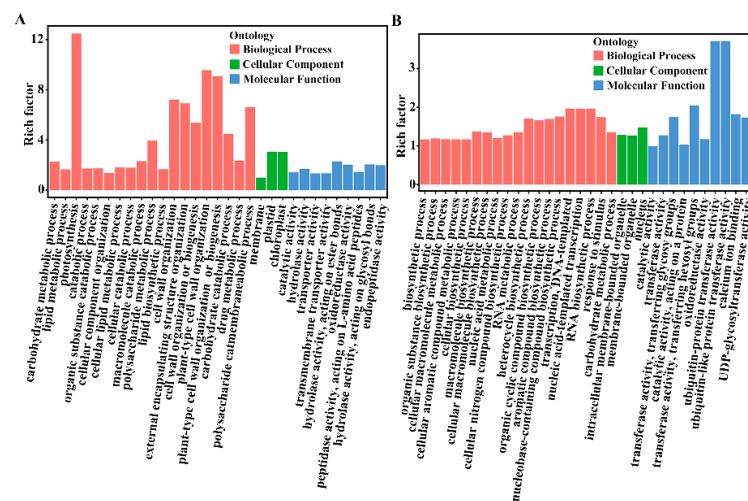


Figure 7. GO classification of all commonly upregulated and downregulated DEGs in blueberry fruits in 2021. GO classification of co-upregulated genes (A). GO classification of co-downregulated genes (B).

3.3. Differential Expression Analysis of Candidate Genes Related to Anthocyanins Synthesis and Metabolism

In the RNA-seq results, we selected 39 DEGs associated with anthocyanin synthesis (Figure 8). These genes include key structural genes in the anthocyanin biosynthesis pathway (Figure 9A) and transcription factors such as MYB, bHLH, and WD40 family.

Heat map results showed that nine genes were upregulated twice in the RNA-seq results and 13 genes were downregulated twice in RNA-seq results (Figure 8). To confirm the repeatability and accuracy of the RNA-seq results in the KEGG pathway, 12 DEGs related to anthocyanin biosynthesis were randomly selected for qRT-PCR analysis. In Figure 9B, the expression levels of six key structural genes involved in anthocyanin synthesis were significantly higher in light stripes than in dark stripes, while the expression levels of *Vc4CL7-2*, *VcCHS*, and *VcDFR* were the opposite. Figure 9C shows that the expression levels of two bHLH family genes, *VcbHLH21* and *VcbHLH25*, and two MYB family genes, *VcMYB108* and *VcMYB7*, were significantly higher in dark stripes than in light stripes. In addition, there are two genes in the bHLH family that are not significantly different in expression. This is consistent with the results of RNA-seq. These results indicated that our transcriptome data were highly reproducible and reliable and could be used for further studies of the key genes involved in anthocyanin accumulation in fruit stripes.

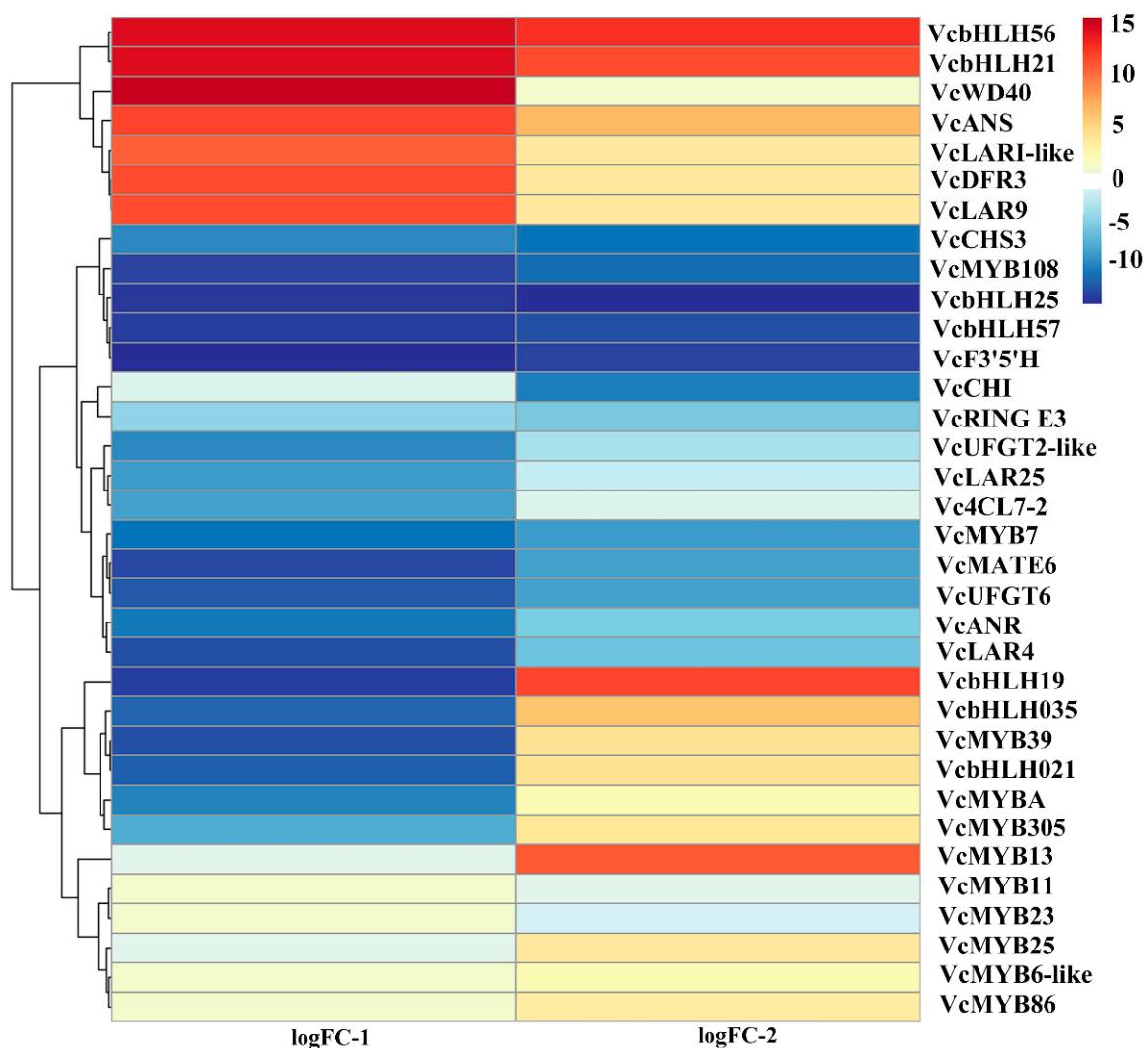


Figure 8. Heat map of anthocyanin synthesis-related DEGs in blueberry peel. LogFC–1 and LogFC–2 (fold change) values were the results of two RNA-seq of blueberry peel. The scale bar indicates upregulated (red) and downregulated (blue) DEGs.

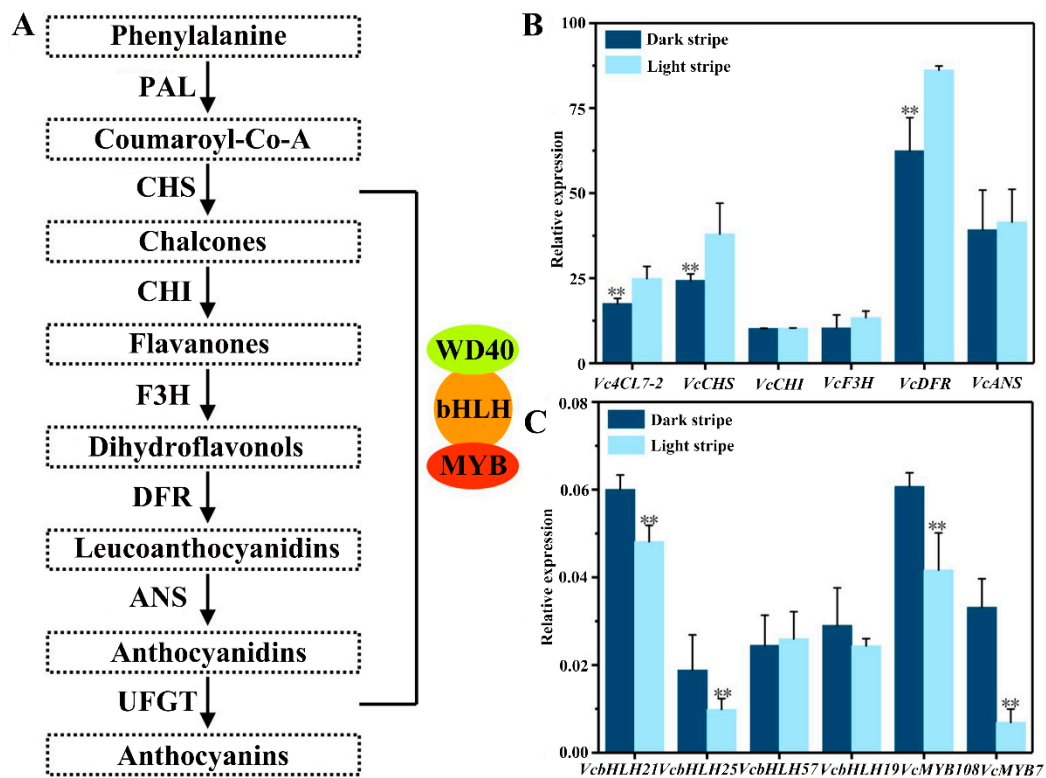


Figure 9. Schematic representation of the anthocyanins biosynthetic pathway in blueberry (A). qRT-PCR validation of six structural genes in dark and light stripes of blueberry (B). qRT-PCR validation of six transcription factors (C). For qRT-PCR, we analyzed three biological repeats. The X-axis is different genes. Values represent the mean \pm SE. Statistical significance was determined by Student's *t* test, ** $p < 0.01$.

4. Discussion

The striped appearance of a blueberry peel is an attractive feature, which directly influences consumers' purchase intention. Striped blueberry fruits have been shown to be a bud mutant. Bud mutants have traditionally been used to study the molecular mechanisms underlying anthocyanin biosynthesis. The fruit of striped blueberry bud mutants were used in this experiment.

Anthocyanin content measurements suggested that anthocyanin content in the dark stripes was significantly higher than that in the light stripes (Figure 1), similar to the observations in striped apple fruit peels [25]. The red regions of apple fruit with stripes contain more anthocyanins and a higher UFGaT activity than adjacent regions from the same fruit [29]. This is explained by reduced/increased transcript levels of all the anthocyanin pathway genes evaluated, including the structural genes in the pathway and transcription factor, which regulates them. A previous study suggested that differences in flavonoid content in blueberry plants may occur naturally in different varieties [30], but differences in flavonoid content in dark and light streaks in the skin of the same variety of blueberries have not been reported at the molecular level. To our knowledge, this is the first comparative transcriptome analysis of the different stripes of the peel of the same blueberry variety. Transcription levels of anthocyanin genes correlate with fruits' stripe patterns. Studies have shown that pigment patterns in apple peels may be a control mechanism, and green stripes are associated with a lower anthocyanin accumulation, which is due to the reduced transcription levels of all the assessed anthocyanin pathway genes, including structural genes [25]. Moreover, the transcription factor MYB10 also plays an important role in stripe formation in apple peels [31]. An overexpression of VcMIR156a in tomato (*Solanum lycopersicum*) enhanced anthocyanin biosynthesis and chlorophyll degradation in the stem

by altering pigment-associated gene expression [32]. *ASR* overexpression could promote strawberry fruit coloring [33]. Anthocyanin accumulation and anthocyanin structural gene expression were correlated with *MYBA* expression, and *MYBA* was able to transactivate the *DFR* promoter from blueberry and other species [34]. Here, the expression of *4CL*, *DFR*, *CHS*, *bHLH21*, *bHLH25*, *MYB108*, and *MYB7* differed between the light and dark stripes (Figure 9), which suggests that they may be the candidate factors most likely to participate in blueberry peel color formation. DNA methylation is one of the most common forms of the covalent modification of eukaryotic genomes. In eukaryotes, DNA methylation refers to the addition of a methyl group to the cytosine 5 carbon site [35,36]. In recent years, the effect of DNA methylation on the growth and development of plant fruits has been widely reported and involved in various aspects of growth and development. This suggests that DNA methylation plays an important role in the regulation of fruit development [37,38]. Previous research has shown that the red-color-loss mutation in European pear ‘Max Red Bartlett’ was because of DNA methylation in the *PyMYB10* promoter [39]. In contrast, the mutation in ‘Zaosu’ with green fruit skin to a red morph was associated with DNA de-methylation in the promoter of *PyMYB10*. Thus, DNA methylation or demethylation inhibited or activated the transcription of *PyMYB10*, subsequently suppressing or inducing the expression of key structural genes involved in anthocyanin biosynthesis (e.g., *UFGT*). The striped pigmentation pattern in the mature fruit of ‘Zaosu Red’ correlated well with DNA methylation patterns in the *PyMYB10* promoter. This finding is consistent with those of other studies on striped pigmentation in apples [25] and maize [40]. However, whether methylation or demethylation plays a role in the striped blueberry pattern formation remains unknown.

This study provides a theoretical foundation for understanding the molecular mechanisms of stripes in pericarps. However, the specific genes that cause dark and light streaks in the skin are unknown and will be the focus of future studies.

5. Conclusions

The difference between the dark and light stripes in blueberries was due to anthocyanin content. We performed a transcriptomic analysis to explore the differentially expressed genes involved in anthocyanin synthesis and signal transduction pathways. Our results showed that the expressions of *VcDFR*, *Vc4CL7-4*, and *VcCHS* in the dark stripes were higher than that in the light stripes, leading to a higher anthocyanin content in the dark stripes. In addition, the expression levels of transcription factors related to anthocyanin synthesis (*VcbHLH21*, *VcbHLH25*, *VcMYB108*, and *VcMYB7*) were higher in dark stripes than in light stripes. Our study identified key genes related to anthocyanin biosynthesis in blueberries and provided a wide range of resources for potential genetic and functional genome studies of non-model plant species.

Supplementary Materials: The following supporting information can be downloaded at: <https://www.mdpi.com/article/10.3390/horticulturae9091036/s1>, Figure S1: Dark and light stripes RPKM box diagram; Figure S2: The volcano plot of differential expressed genes in twice sequencing in 2021; Figure S3: Enrichment of the top 20 GO pathways of all DEGs according to the *p*-value; Table S1: Primer sequences of DEGs for qRT-PCR.

Author Contributions: Z.M. contributed to the writing of the manuscript, experimental method, and analysis of experimental data. Y.Y. analyzed the experimental data. A.Y. and Y.X. participated in RNA extraction. C.L. provided testing materials and supervision. H.Y. was involved in writing, reviewing and editing. All authors have read and agreed to the published version of the manuscript.

Funding: This work was funded by National Grape Industry Technology System (CARS-29), Discipline construction plan of Liaoning Academy of Agricultural Sciences: Small berry breeding and cultivation (2019DD164924), and the Development Program of China Agricultural University (2022-ZZDS-12).

Data Availability Statement: The data that support the findings of this study are available from the corresponding author, (Hui Yuan), upon reasonable request.

Conflicts of Interest: The authors declare no conflict of interest.

References

- Gupta-Elera, G.; Garrett, A.; Martinez, A.; Kraus, R.; Robison, R.; O'Neill, K. A Comparison of Antioxidant Properties in Organic and Conventional Blueberries. *J. Food Res.* **2012**, *1*, 1–7. [[CrossRef](#)]
- An, H.S.; Zhang, J.Y.; Xu, F.J.; Jiang, S.; Zhang, X.Y. Transcriptomic profiling and discovery of key genes involved in adventitious root formation from green cuttings of highbush blueberry (*Vaccinium corymbosum* L.). *BMC Plant Biol.* **2020**, *20*, 182. [[CrossRef](#)] [[PubMed](#)]
- Li, S.; Zhang, J.; Zhang, L.; Fang, X.; Luo, J.; An, H.; Zhang, X. Genome-wide identification and comprehensive analysis reveals potential roles of long non-coding RNAs in fruit development of southern highbush blueberry (*Vaccinium corymbosum* L.). *Front. Plant Sci.* **2022**, *13*, 1078085. [[CrossRef](#)] [[PubMed](#)]
- Zhu, L.C.; Liu, X.; Tan, J.; Wang, B.C. Influence of Harvest Season on Antioxidant Activity and Constituents of Rabbiteye Blueberry (*Vaccinium ashei*) Leaves. *J. Agric. Food Chem.* **2013**, *61*, 11477–11483. [[CrossRef](#)] [[PubMed](#)]
- Sun, W.; Li, X.; Huang, H.; Wei, J.; Zeng, F.; Huang, Y.; Sun, Q.; Miao, W.; Tian, Y.; Li, Y.; et al. Mutation of CsARC6 affects fruit color and increases fruit nutrition in cucumber. *Theor. Appl. Genet.* **2023**, *136*, 150. [[CrossRef](#)]
- Ai, T.N.; Naing, A.H.; Arun, M.; Lim, S.H.; Kim, C.K. Sucrose-induced anthocyanin accumulation in vegetative tissue of Petunia plants requires anthocyanin regulatory transcription factors. *Plant Sci.* **2016**, *252*, 144–150. [[CrossRef](#)]
- Ma, Y.Y.; Ma, X.; Gao, X.; Wu, W.L.; Zhou, B. Light Induced Regulation Pathway of Anthocyanin Biosynthesis in Plants. *Int. J. Mol. Sci.* **2021**, *22*, 11116. [[CrossRef](#)]
- Khoo, H.E.; Azlan, A.; Tang, S.T.; Lim, S.M. Anthocyanidins and anthocyanins: Colored pigments as food, pharmaceutical ingredients, and the potential health benefits. *Food Nutr. Res.* **2017**, *61*, 1361779. [[CrossRef](#)]
- Liu, H.; Liu, Z.; Wu, Y.; Zheng, L.; Zhang, G. Regulatory Mechanisms of Anthocyanin Biosynthesis in Apple and Pear. *Int. J. Mol. Sci.* **2021**, *22*, 8441. [[CrossRef](#)]
- Liu, X.Q.; Yang, W.Z.; Mu, B.N.; Li, S.Z.; Li, Y.; Zhou, X.J.; Zhang, C.Y.; Fan, Y.L.; Chen, R.M. Engineering of 'Purple Embryo Maize' with a multigene expression system derived from a bidirectional promoter and self-cleaving 2A peptides. *Plant Biotechnol. J.* **2018**, *16*, 1107–1109. [[CrossRef](#)]
- Yan, Y.F.; Pico, J.; Gerbrandt, E.M.; Dossett, M.; Castellarin, S.D. Comprehensive anthocyanin and flavonol profiling and fruit surface color of 20 blueberry genotypes during postharvest storage. *Postharvest Biol. Technol.* **2023**, *199*, 112274. [[CrossRef](#)]
- Nie, Q.X.; Feng, L.; Hu, J.L.; Wang, S.A.; Chen, H.H.; Huang, X.J.; Nie, S.P.; Xiong, T.; Xie, M.Y. Effect of fermentation and sterilization on anthocyanins in blueberry. *J. Sci. Food Agric.* **2017**, *97*, 1459–1466. [[CrossRef](#)]
- Li, D.N.; Meng, X.J.; Li, B. Profiling of anthocyanins from blueberries produced in China using HPLC-DAD-MS and exploratory analysis by principal component analysis. *J. Food Compos. Anal.* **2016**, *47*, 1–7. [[CrossRef](#)]
- Borges, G.; Degeneve, A.; Mullen, W.; Crozier, A. Identification of flavonoid and phenolic antioxidants in black currants, blueberries, raspberries, red currants, and cranberries. *J. Agric. Food Chem.* **2010**, *58*, 3901–3909. [[CrossRef](#)] [[PubMed](#)]
- Grace, M.H.; Xiong, J.; Esposito, D.; Ehlenfeldt, M.; Lila, M.A. Simultaneous LC-MS quantification of anthocyanins and non-anthocyanin phenolics from blueberries with widely divergent profiles and biological activities. *Food Chem.* **2018**, *277*, 336–346. [[CrossRef](#)] [[PubMed](#)]
- Mustafa, A.M.; Angeloni, S.; Abouelenein, D.; Acquaticci, L.; Xiao, J.B.; Sagratini, G.; Maggi, F.; Vittori, S.; Caprioli, G. A new HPLC-MS/MS method for the simultaneous determination of 36 polyphenols in blueberry, strawberry and their commercial products and determination of antioxidant activity. *Food Chem.* **2021**, *367*, 130746. [[CrossRef](#)]
- Pertuzatti, P.B.; Barcia, M.T.; Gomez-Alonso, S.; Godoy, H.T.; Hermosin-Gutierrez, I. Phenolics profiling by HPLC-DAD-ESI-MSn aided by principal component analysis to classify Rabbiteye and Highbush blueberries. *Food Chem.* **2021**, *340*, 127958. [[CrossRef](#)]
- Hu, S.Y.; Wang, W.T.; Zhang, C.J.; Zhou, W.; Yan, P.D.; Xue, X.S.; Tian, Q.; Wang, D.H.; Niu, J.F.; Wang, S.Q.; et al. Integrated transcriptomic and metabolomic profiles reveal anthocyanin accumulation in *Scutellaria baicalensis* petal coloration. *Ind. Crops Prod.* **2023**, *194*, 116144. [[CrossRef](#)]
- Cai, J.; Lv, L.T.; Zeng, X.F.; Zhang, F.; Chen, Y.L.; Tian, W.L.; Li, J.R.; Li, X.Y.; Li, Y. Integrative Analysis of Metabolomics and Transcriptomics Reveals Molecular Mechanisms of Anthocyanin Metabolism in the Zikui Tea Plant (*Camellia sinensis* cv. Zikui). *Int. J. Mol. Sci.* **2022**, *23*, 4780. [[CrossRef](#)]
- Jun, J.H.; Xiao, X.R.; Rao, X.L.; Dixon, R.A. Proanthocyanidin subunit composition determined by functionally diverged dioxygenases. *Nat. Plants* **2018**, *4*, 1034–1043. [[CrossRef](#)]
- Zhu, J.Y.; Guo, X.Y.; Li, X.; Tang, D.Q. Composition of Flavonoids in the Petals of Freesia and Prediction of Four Novel Transcription Factors Involving in Freesia Flavonoid Pathway. *Front Plant Sci.* **2021**, *12*, 756300. [[CrossRef](#)] [[PubMed](#)]
- Liang, X.X.; Gao, M.L.; Amanullah, S.; Guo, Y.; Xu, H.G.; Liu, X.S.; Liu, X.J.; Liu, J.X.; Gao, Y.; Yuan, C.Z.; et al. Molecular mapping of candidate gene regulating fruit stripe trait in watermelon. *Euphytica* **2022**, *218*, 174. [[CrossRef](#)]
- Zhai, R.; Wang, Z.G.; Yang, C.Q.; Lin-Wang, K.; Espley, R.; Liu, J.L.; Li, X.Y.; Wu, Z.Y.; Li, P.M.; Guan, Q.M.; et al. PbGA2ox8 induces vascular-related anthocyanin accumulation and contributes to red stripe formation on pear fruit. *Hortic. Res.* **2019**, *6*, 137. [[CrossRef](#)] [[PubMed](#)]
- Telias, A.; Kui, L.W.; Stevenson, D.E.; Cooney, J.M.; Hellens, R.P.; Allan, A.C.; Hoover, E.E.; Bradeen, J.M. Apple skin patterning is associated with differential expression of MYB10. *BMC Plant Biol.* **2011**, *11*, 93. [[CrossRef](#)]

25. Zheng, J.; An, Y.Y.; Wang, L.J. 24-Epibrassinolide enhances 5-ALA-induced anthocyanin and flavonol accumulation in calli of “Fuji” apple flesh. *Plant Cell Tiss. Org.* **2018**, *134*, 319–330. [[CrossRef](#)]
26. Ma, Z.; Cheng, Y. Methods for the chemical determination of anthocyanin on the surface of apple fruit. *China Fruits* **1984**, *4*, 49–51.
27. Li, T.; Li, X.; Tan, D.; Jiang, Z.; Wei, Y.; Li, J.; Du, G.; Wang, A. Distinct expression profiles of ripening related genes in the “Nanguo” pear (*Pyrus ussuriensis*) fruits. *Sci. Hortic.* **2014**, *71*, 78–82. [[CrossRef](#)]
28. Tan, D.; Li, T.; Wang, A. Apple 1-Aminocyclopropane-1-Carboxylic Acid Synthase Genes, MdACS1 and MdACS3a, are Expressed in Different Systems of Ethylene Biosynthesis. *Plant Mol. Biol. Rep.* **2013**, *31*, 204–209. [[CrossRef](#)]
29. Ju, Z.G.; Liu, C.L.; Yuan, Y.B.; Wang, Y.Z.; Liu, G.S. Coloration potential, anthocyanin accumulation, and enzyme activity in fruit of commercial apple cultivars and their F1 progeny. *Sci. Hortic.* **1999**, *79*, 39–50. [[CrossRef](#)]
30. Burdulis, D.; Sarkinas, A.; Jasutiene, I.; Stackeviciene, E.; Nikolajevas, L.; Janulis, V. Comparative Study of Anthocyanin Composition, Antimicrobial and Antioxidant Activity in bilberry (*Vaccinium myrtillus* L.) and Blueberry (*Vaccinium corymbosum* L.) Fruits. *ACTA Pol. Pharm.* **2009**, *66*, 399–408.
31. Lin-Wang, K.; Micheletti, D.; Palmer, J.; Volz, R.; Lozano, L.; Espley, R.; Hellens, R.P.; Chagne, D.; Rowan, D.D.; Troggo, M.; et al. High temperature reduces apple fruit colour via modulation of the anthocyanin regulatory complex. *Plant Cell Environ.* **2011**, *34*, 1176–1190. [[CrossRef](#)] [[PubMed](#)]
32. Li, X.Y.; Hou, Y.M.; Xie, X.; Li, H.X.; Li, X.D.; Zhu, Y.; Zhai, L.L.; Zhang, C.Y.; Bian, S.M. Blueberry MIR156a/SPL12 module coordinates the accumulation of chlorophylls and anthocyanins during fruit ripening. *J. Exp. Bot.* **2020**, *71*, 5976–5989. [[CrossRef](#)] [[PubMed](#)]
33. Liu, Z.J.; Zhao, P.C.; Cui, L.W.; Fang, J.G.; Jia, H.F. Over-expression of Gene FaASR Promotes Strawberry Fruit Coloring. *Hortic. Plant J.* **2015**, *1*, 147–154.
34. Plunkett, B.J.; Espley, R.V.; Dare, A.P.; Warren, B.W.; Grierson, E.R.P.; Cordiner, S.; Turner, J.L.; Allan, A.C.; Albert, N.W.; Davies, K.M.; et al. MYBA From Blueberry (*Vaccinium* Section *Cyanococcus*) Is a Subgroup 6 Type R2R3MYB Transcription Factor That Activates Anthocyanin Production. *Front. Plant Sci.* **2018**, *9*, 1300. [[CrossRef](#)] [[PubMed](#)]
35. Law, J.A.; Jacobsen, S.E. Establishing, maintaining and modifying DNA methylation patterns in plants and animals. *Nat. Rev. Genet.* **2010**, *11*, 204–220. [[CrossRef](#)]
36. He, G.M.; Elling, A.A.; Deng, X.W. The Epigenome and Plant Development. *Annu. Rev. Plant Biol.* **2011**, *62*, 411–435. [[CrossRef](#)]
37. Huang, H.; Liu, R.E.; Niu, Q.F.; Tang, K.; Zhang, B.; Zhang, H.; Chen, K.S.; Zhu, J.K.; Lang, Z.B. Global increase in DNA methylation during orange fruit development and ripening. *Proc. Natl. Acad. Sci. USA* **2019**, *116*, 1430–1436. [[CrossRef](#)]
38. Liu, Z.Y.; Wu, X.T.; Liu, H.W.; Zhang, M.L.; Liao, W.B. DNA methylation in tomato fruit ripening. *Physiol. Plant.* **2022**, *174*, e13627. [[CrossRef](#)]
39. Wang, Z.; Meng, D.; Wang, A.; Li, T.; Jiang, S.; Cong, P.; Li, T. The methylation of PcMYB10 promoter is associated with green skinned sport in “Max Red Bartlett” pear. *Plant Physiol.* **2013**, *162*, 885–896. [[CrossRef](#)]
40. Cocciolone, S.M.; Cone, K.C. Pl-Bh, an anthocyanin regulatory gene of maize that leads to variegated pigmentation. *Genetics* **1993**, *135*, 575–588. [[CrossRef](#)]

Disclaimer/Publisher’s Note: The statements, opinions and data contained in all publications are solely those of the individual author(s) and contributor(s) and not of MDPI and/or the editor(s). MDPI and/or the editor(s) disclaim responsibility for any injury to people or property resulting from any ideas, methods, instructions or products referred to in the content.